Journal of Sound and Vibration (2001) **243**(1), 145–155
doi:10.1006/jsvi.2000.3413, available online at http://www.idealibrary.com on IDEAL®

ROBUST H_∞ VIBRATION CONTROL FOR FLEXIBLE LINKAGE MECHANISM SYSTEMS WITH PIEZOELECTRIC SENSORS AND ACTUATORS

X. ZHANG, C. SHAO, S. LI AND D. XU

Mechatronic Engineering Department, Shantou University, Shantou, Guangdong 515063, *People's Republic of China. E-mail: xmzhang@stu.edu.cn or xmzhang@me.umn.edu*

AND

A. G. ERDMAN

Department of Mechanical Engineering, University of Minnesota, 111 *Church Street, Minneapolis, MN* 55455, *U.S.A.*

(*Received* 25 *July* 2000, *and in final form* 24 *November* 2000)

It is well known that the unmodelled dynamics may deteriorate the efficiency of a controller if the controller is not robust enough. This paper presents a robust H_∞ vibration control method for high-speed flexible linkage mechanism systems with piezoelectric actuators and sensors. The robust H_∞ controller is designed based on the complex mode and the H_∞ control theory. The numerical simulation shows that the vibration can be significantly suppressed with permitted actuator voltages by the controller. The robust H_∞ controller can avoid the spillover due to mode truncation to compare with some other method.

1. INTRODUCTION

Mechanisms are now being required to run at higher speeds while maintaining positioning accuracy. Because of the higher operating speeds, the mechanisms need to be made as lightweight as possible to reduce the inertial forces, and consequently, the driving torque requirements. However, the lighter members are more likely to elastically vibrate due to the inertial and external forces. Recently, considerable attention has been paid to the investigations of the vibration control of flexible mechanisms in order to achieve high-speed and lightweight machines with accurate performances. Heretofore, there are basically five design philosophies, which have been developed to improve the elastodynamic responses. The first involves designing links in the conventional materials with optimization of the cross-sectional geometry of the members [1, 2]. The second one uses additional damping materials to dissipate the vibration energy [3–5]. The third advocates that the mechanism links should be built of advanced composite materials because of their high damping and high stiffness-to-weight ratio [6, 7]. These three design concepts may be referred to as passive vibration control. The fourth introduces a microprocessor-controlled actuator into the original mechanism to reduce the deflection of the flexible linkage [8–10]. The last involves the application of smart materials featuring distributed actuators and sensors to the linkage mechanisms [11–18] or in some structures [19–21] to control unwanted vibration. Sung and Chen [11] attempted to control the elastodynamic response of

0022-460X/01/210145 + 11 $35.00/0

a four-bar linkage mechanism system with a flexible follower, a rigid crank, and a rigid coupler. Two patches of piezoceramic actuators were bonded to the surface of the follower at two locations that are symmetric with respect to its midpoint and one piezoceramic sensor was bonded to the surface of its midpoint. The authors assumed that the free vibration modes of the flexible follower link were the same as those of a simply supported beam. Optimal linear quadratic regulator (LQR) is employed in the control system. Liao and Sung [12] derived the finite element equations of the above mechanism and studied the active vibration control problem both analytically and experimentally based on the linear quadratic Gaussian (LQG) theory. In the work of reference [13], Choi *et al.* investigated a slider-crank mechanism whose flexible connecting rod was bonded with two piezoelectric films to its upper and lower surfaces. One of the films was used as a distributed sensor while the other was used as a distributed actuator. The linear optimal feedback control law with a Luenberger observer was employed. On the basis of the independent modal control method, Zhang *et al.* [14, 15] studied the active vibration control problem for the flexible mechanisms of all whose members were considered as flexible. By means of experimental studies, Thompson and Tao [16] controlled the connecting rod vibrations of a slider-crank mechanism by using two sets of piezoelectric actuator/strain gauge sensor pairs. Classical position feedback controller was employed in the experimental system. Sannah and Smaili [17] presented an experimental investigation on controlling the elastodynamic response of a four-bar mechanism system with a flexible coupler link, slightly less flexible follower link, and relatively rigid crank. A controller, which consists of a LQR and a Luenberger observer, was designed and implemented. However, the state-space matrices of the system were assumed to be constant for the entire motion cycle of the mechanism, which is not the case when the mechanism operates at high speeds. In reference [18], Shao and Zhang develop a hybrid-independent modal controller which is composed of state feedback and disturbance feed-forward control laws. This control strategy can effectively suppress the vibration of the controlled system, but the control spillover may exist if the control is not imputed properly. Except that, Chen and Shen developed an optimal control method for structures with piezoelectric modal sensors and actuators. Peng *et al.* [20], Lam and Ng [21] investigated the active vibration problems for both the composite beams and plates with piezoelectric sensors and actuators.

The aim of this research is to design a robust controller to overcome the phenomenon of spillover for high-speed flexible linkage mechanism systems. It is well known that the H_∞ design technique [22, 23] provides better robustness than LQG, or H_2, method. One of the features of H_∞ control is that the design specifications are given in the frequency domain, and thus it is easy for H_∞ control to deal with the uncertainty at high frequencies, and it is comparably simple to guarantee the robust stability. H_∞ control is receiving intense interest in the control literature and has been successfully applied to a wide variety of practical problems [24, 25]. But in the area of vibration control for high-speed flexible linkage mechanism systems, we have not seen any publications. In this paper, based on the complex mode theory, robust H_∞ controller for active vibration control of the high-speed flexible linkage mechanism systems with piezoelectric actuators and sensors is investigated. The numerical computation carried out on a four-bar linkage mechanism shows that the vibration of the system is significantly suppressed with permitted actuator voltages and the spillovers due to mode truncation are avoided.

2. MODELLING OF CONTROL

According to the Hamilton theory, the mathematical model of control for the flexible linkage mechanism can be expressed as [18]

$$\mathbf{M}\ddot{\mathbf{q}} + \mathbf{C}\dot{\mathbf{q}} + \mathbf{K}\mathbf{q} = \mathbf{P} - \mathbf{D}_a\mathbf{u}, \tag{1}$$

$$\mathbf{y} = \mathbf{D}_s\,\mathbf{q}, \tag{2}$$

where $\mathbf{M}$, $\mathbf{C}$, $\mathbf{K}$, $\mathbf{D}_a$, and $\mathbf{D}_s$ are the systematic mass, damping, stiffness, control and output matrices, respectively, and $\mathbf{P}$ is the systematic generalized force vector, $\mathbf{q}$, $\dot{\mathbf{q}}$, $\ddot{\mathbf{q}}$ are the generalized displacement, velocity, and acceleration vectors of the linkage system, respectively, $\mathbf{u}$ is the control input vector, and $\mathbf{y}$ is the output vector of the sensors. This model includes both the rigid-body and the elastic motion coupling terms and the elastodynamics and piezoelectricity coupling terms, and takes into account the effects of the piezoelectric apparatus upon the mass and the stiffness of the system. It is noted that all the system matrices are not constant but periodically varying functions of the position of each links of the mechanism. Matrices $\mathbf{C}$ and $\mathbf{K}$ are not symmetric matrices, so it cannot be solved using the traditional real modal method. In order to decouple equation (1), we define a state-space vector as

$$\bar{\mathbf{x}} = \{\dot{\mathbf{q}}^{\mathrm{T}}, \mathbf{q}^{\mathrm{T}}\}^{\mathrm{T}}, \dot{\bar{\mathbf{x}}} = \{\ddot{\mathbf{q}}^{\mathrm{T}}, \dot{\mathbf{q}}^{\mathrm{T}}\}^{\mathrm{T}}.$$

Rewriting equations (1) and (2) in terms of the state-space vector yields

$$\bar{\mathbf{A}}\dot{\bar{\mathbf{x}}} + \bar{\mathbf{B}}\bar{\mathbf{x}} = \mathbf{w}_0 + \bar{\mathbf{D}}\mathbf{u}, \tag{3}$$

$$\mathbf{y} = \mathbf{S}\bar{\mathbf{x}}, \tag{4}$$

where

$$\bar{\mathbf{A}} = \begin{bmatrix} \mathbf{0} & \mathbf{M} \\ \mathbf{M} & \mathbf{C} \end{bmatrix}, \qquad \bar{\mathbf{B}} = \begin{bmatrix} -\mathbf{M} & \mathbf{0} \\ \mathbf{0} & \mathbf{K} \end{bmatrix}, \qquad \mathbf{w}_0 = \begin{Bmatrix} \mathbf{0} \\ \mathbf{P} \end{Bmatrix}, \qquad \bar{\mathbf{D}} = -\begin{Bmatrix} \mathbf{0} \\ \mathbf{D}_a \end{Bmatrix}, \qquad \mathbf{S} = [\mathbf{0},\ \mathbf{D}_s].$$

If the complex eigenvalues $\lambda_i = \lambda_{iR} \pm j\lambda_{il}$, $i = 1, 2, \ldots, n$, where n is the number of the generalized co-ordinates of the system, and the corresponding normalized left eigenvectors $\mathbf{X}'_i = \mathbf{X}'_{iR} \pm \mathrm{j}\mathbf{X}'_{il}$ and the right eigenvectors $\mathbf{X}_i = \mathbf{X}_{iR} \pm \mathrm{j}\mathbf{X}_{il}$ are known, a linear transformation can be performed, based on the complex modal space basis. Let

$$\mathbf{X}' = [\ldots, \mathbf{X}'_{iR}, \mathbf{X}'_{il}, \ldots], \qquad \mathbf{X} = 2[\ldots, \mathbf{X}_{iR}, -\mathbf{X}_{il}, \ldots], \quad i = 1, \ldots, n.$$

The transformation is

$$\bar{\mathbf{x}} = \mathbf{X}\mathbf{x}_0, \tag{5}$$

where $\mathbf{x}_0 = (\ldots, \mathbf{x}_{iR},\ \mathbf{x}_{il}, \ldots)^{\mathrm{T}}$. Substituting equation (5) into equations (3) and (4), premultiplying equation (3) by $\mathbf{X}'$ yields

$$\dot{\mathbf{x}}_0 = \mathbf{A}_0\mathbf{x}_0 + \mathbf{B}_{10}\mathbf{w}_0 + \mathbf{B}_{20}\mathbf{u}, \tag{6}$$

$$\mathbf{y} = \mathbf{C}_{20}\mathbf{x}_0, \tag{7}$$

where

$$\mathbf{A}_0 = \text{Block diag.}\,(\ldots \mathbf{A}_{ii} \ldots), \qquad \mathbf{A}_{ii} = \begin{bmatrix} \lambda_{iR} & -\lambda_{il} \\ \lambda_{il} & \lambda_{iR} \end{bmatrix},$$

$$\mathbf{B}_{10} = \mathbf{X}'^{\mathrm{T}}, \qquad \mathbf{B}_{20} = \mathbf{X}'^{\mathrm{T}}\mathbf{D}, \qquad \mathbf{C}_{20} = \mathbf{S}\mathbf{X}.$$

From the control theory one can control an equivalent number c of vibrational modes and leave a number r of residual uncontrollable modes with $r + c = n$. Let

$$\mathbf{x}_0 = \{\mathbf{x}_c^{\mathrm{T}} \quad \mathbf{x}_r^{\mathrm{T}}\}^{\mathrm{T}}.$$

Equations (6) and (7) can be rewritten as

$$\begin{Bmatrix} \dot{\mathbf{x}}_c \\ \dot{\mathbf{x}}_r \end{Bmatrix} = \begin{bmatrix} \mathbf{A}_c & \mathbf{0} \\ \mathbf{0} & \mathbf{A}_r \end{bmatrix} \begin{Bmatrix} \mathbf{x}_c \\ \mathbf{x}_r \end{Bmatrix} + \begin{bmatrix} \mathbf{B}_{1c} \\ \mathbf{B}_{1r} \end{bmatrix} \mathbf{w}_0 + \begin{bmatrix} \mathbf{B}_{2c} \\ \mathbf{B}_{2r} \end{bmatrix} \mathbf{u}, \tag{8}$$

$$\mathbf{y} = [\mathbf{C}_{2c} \quad \mathbf{C}_{2r}] \begin{Bmatrix} \mathbf{x}_c \\ \mathbf{x}_r \end{Bmatrix}. \tag{9}$$

3. THE ROBUST H_∞ CONTROLLER DESIGN

The aim of this section is to design a controller

$$\mathbf{u} = \mathbf{G}\mathbf{y} \tag{10}$$

which satisfies the conditions: (1) the closed-loop system is stable, and (2) when the initial state vector $\bar{\mathbf{x}}(0) = \mathbf{0}$, then at any time t, the system satisfies the following relation:

$$J = \int_0^t (\bar{\mathbf{x}}^{\mathrm{T}}\mathbf{Q}\bar{\mathbf{x}} + \mathbf{u}^{\mathrm{T}}\mathbf{R}\mathbf{u})\,\mathrm{d}t < \varepsilon \int_0^t \mathbf{w}_0^{\mathrm{T}}\mathbf{w}_0\,\mathrm{d}t, \tag{11}$$

where ε is a given constant, $\mathbf{Q}$ and $\mathbf{R}$ are the weighting matrices. Define the controlled output vector as

$$\mathbf{z}_0 = \mathbf{N}\bar{\mathbf{x}} + \mathbf{L}\mathbf{u} = \mathbf{C}_{1c}\mathbf{x}_c + \mathbf{D}_{12c}\mathbf{u}, \tag{12}$$

where

$$\mathbf{Q} = \mathbf{N}^{\mathrm{T}}\mathbf{N}, \qquad \mathbf{R} = \mathbf{L}^{\mathrm{T}}\mathbf{L}, \qquad \mathbf{C}_{1c} = \mathbf{N}\mathbf{X}_c, \qquad \mathbf{D}_{12c} = \mathbf{L}.$$

The equivalent form of equation (11) is

$$\|\mathbf{T}_{z_0 w_0}\|_\infty < \gamma = \sqrt{\varepsilon}, \tag{13}$$

where $\mathbf{T}_{z_0 w_0}$ is the closed-loop transfer function from $\mathbf{w}_0$ to $\mathbf{z}_0$, $\|\bullet\|_\infty$ indicates the H_∞ norm. Rewriting equations (8) and (9) in the transfer function form

$$\begin{Bmatrix} \mathbf{z}_0 \\ \mathbf{y} \end{Bmatrix} = \begin{bmatrix} \mathbf{P}_{11} & \mathbf{P}_{12} \\ \mathbf{P}_{21} + \Delta\mathbf{P}_{21} & \mathbf{P}_{22} + \Delta\mathbf{P}_{22} \end{bmatrix} \begin{Bmatrix} \mathbf{w}_0 \\ \mathbf{u} \end{Bmatrix},$$

where

$$\mathbf{P}_{11} = \mathbf{C}_{1c}(s\mathbf{I} - \mathbf{A}_c)^{-1}\mathbf{B}_{1c}, \qquad \mathbf{P}_{12} = \mathbf{C}_{1c}(s\mathbf{I} - \mathbf{A}_c)^{-1}\mathbf{B}_{2c} + \mathbf{D}_{12c},$$

$$\mathbf{P}_{21} = \mathbf{C}_{2c}(s\mathbf{I} - \mathbf{A}_c)^{-1}\mathbf{B}_{1c}, \qquad \Delta\mathbf{P}_{21} = \mathbf{C}_{2r}(s\mathbf{I} - \mathbf{A}_r)^{-1}\mathbf{B}_{1r},$$

$$\mathbf{P}_{22} = \mathbf{C}_{2c}(s\mathbf{I} - \mathbf{A}_c)^{-1}\mathbf{B}_{2c}, \qquad \Delta\mathbf{P}_{22} = \mathbf{C}_{2r}(s\mathbf{I} - \mathbf{A}_r)^{-1}\mathbf{B}_{2r}.$$

We know that there are uncertainties, $\Delta\mathbf{P}_{22}$ between the full model and the reduced model in the frequency domain, which are the main reasons to cause spillover. Introduce the suppositional evaluation output $\mathbf{z}_W = \mathbf{W}\mathbf{u}$ and the suppositional input disturbance $\mathbf{w}_W = \Delta \cdot \mathbf{z}_W$, where W is the weighting function, Δ is a co-ordinate matrix which satisfies $\Delta \cdot W = \Delta\mathbf{P}_{22}$, $\|\Delta\|_\infty \leqslant 1$. From reference [22] one knows that the robust stability condition of the closed-loop system is

$$\|\mathbf{T}_{z_W w_W}\|_\infty = \|W\mathbf{H}\|_\infty < 1, \tag{14}$$

where $\mathbf{H}$ is the closed-loop transfer function from the output of $\Delta\mathbf{P}_{22}$ to control the input $\mathbf{u}$ which can be expressed as

$$\mathbf{H} = (I - \mathbf{G}\mathbf{P}_{22})^{-1}\mathbf{G}.$$

If the state form expression of W is $(\mathbf{A}_W, \mathbf{B}_W, \mathbf{C}_W, \mathbf{D}_W)$, then the augmented controlled system can be expressed as

$$\dot{\mathbf{x}} = \mathbf{A}\mathbf{x} + \mathbf{B}_1\mathbf{w} + \mathbf{B}_2\mathbf{u}, \tag{15}$$

$$\mathbf{z} = \mathbf{C}_1\mathbf{x} + \mathbf{D}_{12}\mathbf{u}, \tag{16}$$

$$\mathbf{y} = \mathbf{C}_2\mathbf{x} + \mathbf{D}_{21}\mathbf{w}, \tag{17}$$

where

$$\mathbf{x} = \begin{Bmatrix} \mathbf{x}_c \\ \mathbf{x}_W \end{Bmatrix}, \qquad \mathbf{w} = \begin{Bmatrix} \mathbf{w}_0 \\ \mathbf{w}_W \end{Bmatrix}, \qquad \mathbf{z} = \begin{Bmatrix} \mathbf{z}_0 \\ \mathbf{z}_W \end{Bmatrix},$$

$$\mathbf{A} = \begin{bmatrix} \mathbf{A}_c & \mathbf{0} \\ \mathbf{0} & \mathbf{A}_W \end{bmatrix}, \qquad \mathbf{B}_1 = \begin{bmatrix} \mathbf{B}_{1c} & \mathbf{0} \\ \mathbf{0} & \mathbf{0} \end{bmatrix},$$

$$\mathbf{B}_2 = \begin{bmatrix} \mathbf{B}_{2c} \\ \mathbf{B}_W \end{bmatrix}, \qquad \mathbf{C}_1 = \begin{bmatrix} \mathbf{C}_{1c} & \mathbf{0} \\ \mathbf{0} & \mathbf{C}_W \end{bmatrix}, \qquad \mathbf{D}_{12} = \begin{bmatrix} \mathbf{D}_{12c} \\ \mathbf{D}_W \end{bmatrix},$$

$$\mathbf{C}_2 = [\mathbf{C}_{2c} \quad \mathbf{0}], \qquad \mathbf{D}_{21} = [\mathbf{0} \quad \mathbf{I}].$$

By solving the above standard H_∞ problem, one can obtain the state-space form output feedback robust controller G:

$$\dot{\mathbf{x}}_G = \mathbf{A}_G\mathbf{x}_G + \mathbf{B}_1\mathbf{w} + \mathbf{B}_G\mathbf{y},$$

$$\mathbf{u} = \mathbf{C}_G\mathbf{x}_G, \tag{18}$$

where

$$\mathbf{A}_G = \mathbf{A} + \mathbf{B}_1\mathbf{B}_1^{\mathrm{T}}\mathbf{X} - \mathbf{Z}^{-1}\mathbf{L}\mathbf{C}_2 + \mathbf{B}_2\mathbf{F},$$

$$\mathbf{B}_G = \mathbf{Z}^{-1}\mathbf{L}, \qquad \mathbf{C}_G = \mathbf{E}^{-1}\mathbf{F},$$

$$\mathbf{F} = -\mathbf{B}_2^{\mathrm{T}}\mathbf{X}, \qquad \mathbf{L} = \mathbf{Y}\mathbf{C}_2^{\mathrm{T}}, \qquad \mathbf{Z} = \mathbf{I} - \mathbf{X}\mathbf{Y}.$$

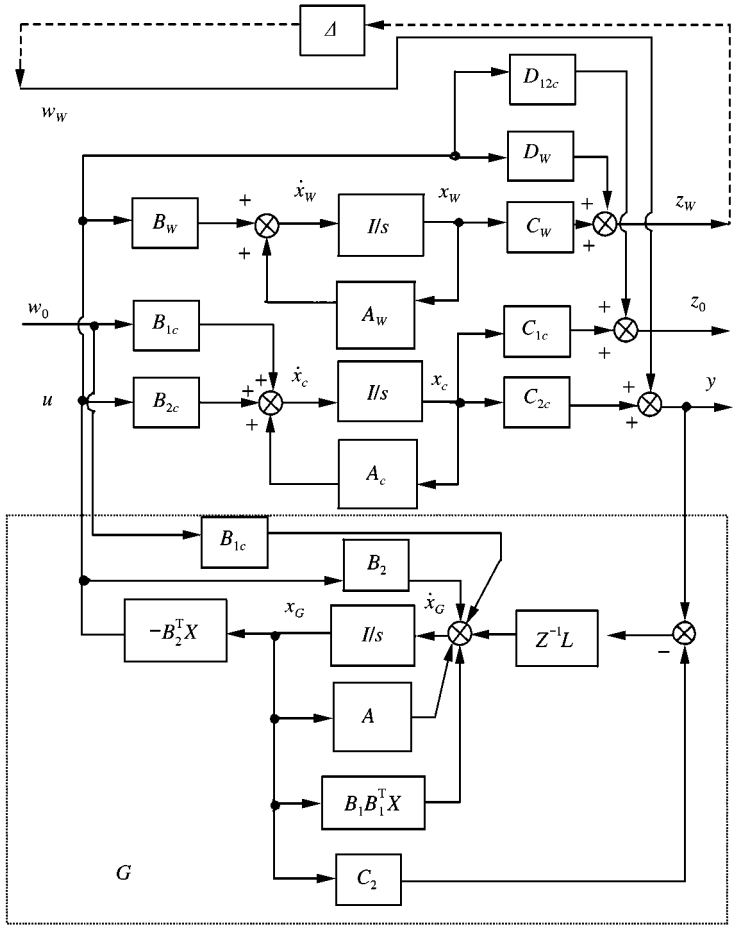

Figure 1. Block diagram of the control system.

Matrix $\mathbf{E}$ is positive definite and satisfies relation $\mathbf{D}_{12}^{\mathrm{T}}\mathbf{D}_{12} = \mathbf{EE}$, $\mathbf{X}$ and $\mathbf{Y}$ are the positive semi-definite solutions of the Riccati equations (19) and (20).

$$\mathbf{A}^{\mathrm{T}}\mathbf{X} + \mathbf{XA} + \mathbf{X}\left(\frac{1}{\varepsilon}\mathbf{B}_1\mathbf{B}_1^{\mathrm{T}} - \mathbf{B}_2\mathbf{B}_2^{\mathrm{T}}\right) + \mathbf{C}_1^{\mathrm{T}}\mathbf{C}_1 = 0, \tag{19}$$

$$\mathbf{AY} + \mathbf{YA}^{\mathrm{T}} + \mathbf{Y}(\mathbf{C}_1^{\mathrm{T}}\mathbf{C}_1 - \mathbf{C}_2^{\mathrm{T}}\mathbf{C}_2)\mathbf{Y} + \frac{1}{\varepsilon}\mathbf{B}_1\mathbf{B}_1^{\mathrm{T}} = 0. \tag{20}$$

The closed-loop equation of the system is

$$\begin{Bmatrix} \dot{\mathbf{x}} \\ \dot{\mathbf{x}}_G \\ \dot{\mathbf{x}}_r \end{Bmatrix} = \begin{bmatrix} \mathbf{A} & \mathbf{B}_2\mathbf{C}_G & \mathbf{0} \\ \mathbf{B}_G\mathbf{C}_{2c} & \mathbf{A}_G & \mathbf{B}_G\mathbf{C}_{2r} \\ \mathbf{0} & \mathbf{B}_{2r}\mathbf{C}_G & \mathbf{A}_r \end{bmatrix} \begin{Bmatrix} \mathbf{x} \\ \mathbf{x}_G \\ \mathbf{x}_r \end{Bmatrix} = \begin{bmatrix} \mathbf{B}_1 \\ \mathbf{B}_1 + \mathbf{B}_G\mathbf{D}_{21} \\ [\mathbf{B}_{1r}\ \mathbf{0}] \end{bmatrix} w. \tag{21}$$

Figure 1 shows the block diagram of the control system.

4. NUMERICAL SIMULATION

In order to demonstrate the validity of the proposed control methodology, a computer simulative analysis is carried out on a four-bar linkage mechanism shown in Figure 2. In this study, all the links are treated as flexible ones. The property parameters of the mechanism and the piezoelectric ceramic actuators and PVDF piezoelectric sensors are the same as that in reference [18]. A pair of actuator and a pair of sensor are bonded on each of the links. The actuator and sensor on the crank link are 30 mm long and 30 mm wide and are located at a quarter and three quarters length of the link while those on the coupler and the follower are 40 mm long and 25 mm wide, and are at their three-eighths and five-eighths length.

In this study, the crank is modelled by two finite elements, and the coupler and the follower are both modelled by four elements. The crank speed is 398 r.p.m., at this speed the mechanism system exists in the lower-order resonance [26]. The first three modes are taken as controlled modes, and damping ratios of the controlled modes are all 0·03.

In the controller design process, the balance between the vibration control level and the control input must be considered because the piezoelectric actuators can only endure limited input voltage. The actuators used in this paper were manufactured from piezoelectric ceramic with thickness of 1 mm (made in acoustics institute of Chinese Academy of Science). The allowable voltage of the piezoelectric actuators used in the four-bar linkage mechanism system is from -500 V to $+500$ V. That is to say the control voltages must not exceed this range, otherwise, the actuators will lose their piezoelectricity and fail to work at all. To satisfy the above requirements, selecting the weighting matrices $\mathbf{Q}$ and $\mathbf{R}$ properly is very important to the robust H_∞ controller design. After a certain amount of trial and error, we selected

$$\mathbf{Q} = diag[\ldots, 10^8, \ldots], \qquad \mathbf{R} = diag[2{\cdot}0,\ 1{\cdot}2,\ 2{\cdot}0], \quad \text{and} \quad \varepsilon_0 = 6{\cdot}4 \times 10^9.$$

In order to meet the frequency domain robustness requirement with respect to the unstructured uncertainty, according to the maximum of $\|\Delta \mathbf{P}_{22}(j\omega)\|_\infty$ in one cycle of operation for the mechanism, after a certain amount of trial and error, we selected the weighting function as follows

$$W = \frac{8{\cdot}0 \times 10^{-13}(s/900 + 1)}{(s/1500)^2 + 2 \times 0{\cdot}02 \times s/1500 + 1}.$$

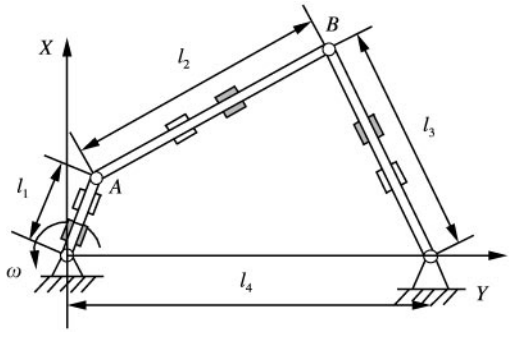

Figure 2. Four-bar linkage ▭ Sensor; ▬ Actuator.

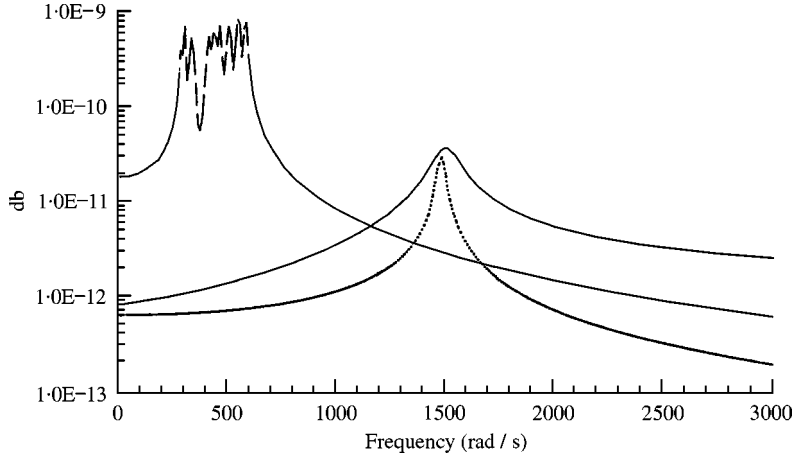

Figure 3. Unmodelled dynamics and weighting function. —, $\|W\|_\infty$; ----, $\|P_{22}(j\omega)\|_\infty$; ·····, $\|\Delta P_{22}(j\omega)\|_\infty$.

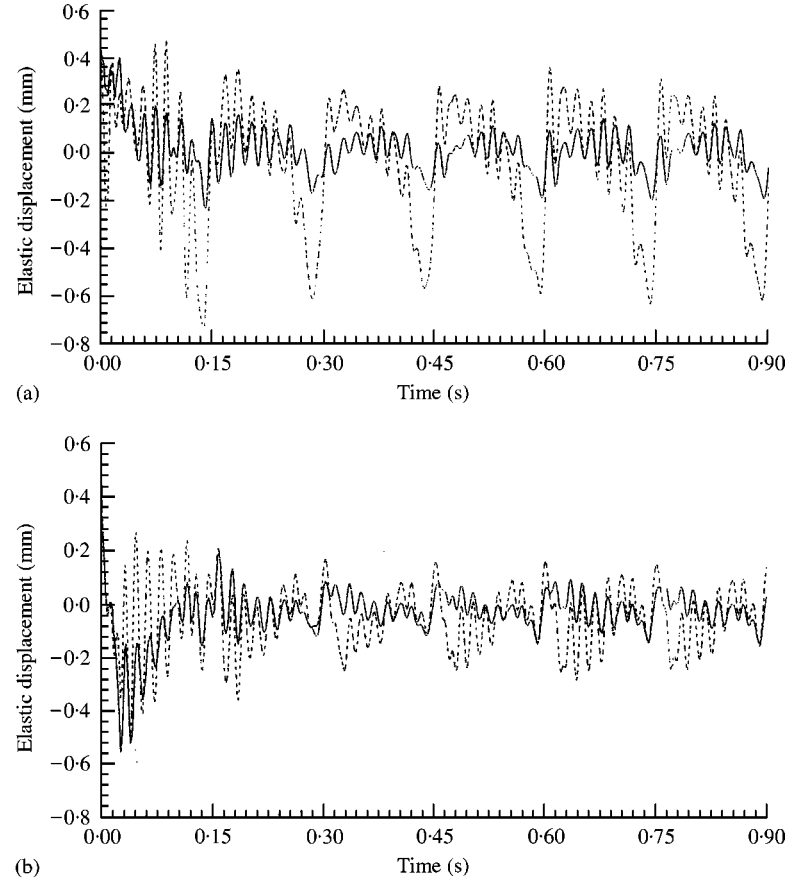

Figure 4. Transient response of the midpoint of the coupler in x direction (a) and in y direction (b): ·····, original system; —, robust H_∞ control.

Figure 3 shows the plots of the weighting function and the maximum of $\|\mathbf{P}_{22}(j\omega)\|_\infty$ and $\|\Delta\mathbf{P}_{22}(j\omega)\|_\infty$ in one cycle of operation for the mechanism. From this figure, one can see that the weighting function is suitable.

Figure 4 shows the transient elastodynamic response of the midpoint of the coupler link both with and without control action. It is seen that the steady-state responses of the mechanism system were significantly suppressed after employing control input. Figure 5 presents the control voltage applied to the piezoelectric actuators of the follower and the coupler. Obviously, the control voltages satisfy the voltage constraints very well.

Figure 6 shows the frequency response of the open-loop and the closed-loop system both by the robust H_∞ control method and the state feedback and disturbance feed-forward control method [18]. From Figure 6, one finds that the frequency response has been entirely changed by the robust H_∞ controller and there is no control spillover existing in the controlled system. Though the responses can be well suppressed by using the feedback and disturbance feed-forward control method, control spillover occurred at the location of the fourth and the fifth modes.

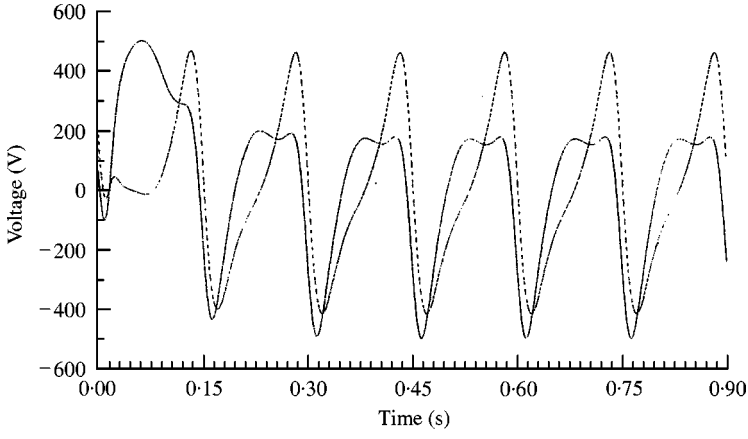

Figure 5. Input voltages of the actuators: ——, follower; - - - - coupler.

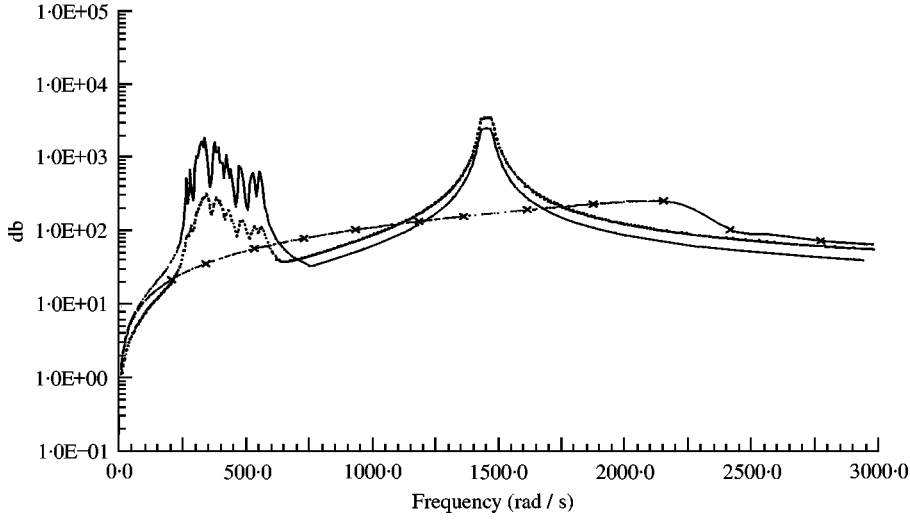

Figure 6. Frequency response: ——, original system; ·····, reduced mode method; —×—, robust H_∞ method.

5. CONCLUSIONS

The robust H_∞ controller for active vibration control of the high-speed flexible linkage mechanism systems with piezoelectric actuators and sensors are investigated. The numerical simulation shows that the vibration of the system is significantly suppressed with permitted actuator voltages using the controller, and the robust H_∞ controller can avoid the spillover due to mode truncation compared with some other methods. The experimental researchers based on the controller will be the aim of our further work.

Properly selecting the weighting matrices **Q** and **R**, and the weighting functions is very important for successfully designing the controller for the system. A certain amount of trial and error iterations are necessary in the design process, this is the main drawback of this method.

ACKNOWLEDGMENTS

This research was supported by the National Natural Science Foundation of China under Grants 59975056, 59605001, the Foundation for University Key Teacher by the Ministry of Education, the Natural Science Foundation of Guangdong Province under Grant 970381, 20000783, and the elitist Foundation of Guangdong Province under Grant 9912. The first author gratefully acknowledges these supports.

REFERENCES

1. W. L. CLEGHORN, F. G. FENTON and B. TABARROK 1981 *Mechanism and Machine Theory* **16**, 339–406. Optimal design of high-speed flexible mechanisms.
2. X. M. ZHANG, Y. SHEN, H. Z. LIU and W. CAO 1995 *Mechanism and Machine Theory* **30**, 131–139. Optimal design of flexible mechanisms with frequency constraints.
3. E. H. EL-DANNAH and S. H. FARGHALY 1993 *Mechanism and Machine Theory* **28**, 447–457. Vibratory response of a sandwich link in a high-speed mechanism.
4. X. M. ZHANG 1999 *Chinese Journal of Mechanical Engineering* **35**, 55–58. Modal loss factor predication in the passive vibration control of elastic mechanism systems.
5. C. SISEMORE, A. SMAILI and R. HOUGHTON 1999 *The* 10*th World Congress on the Theory of Machines and Mechanisms*, *Oulu*, *Finland*, June 20–24, Volume 5, 2140–2145. Passive damping of flexible mechanism systems: experimental and finite element investigations.
6. A. GHAZAVI, F. GARDANINE and N. G. CHALHOUT 1993 *Computers & Structures* **49**, 315–325. Dynamic analysis of a composite material flexible robot arm.
7. C. K. SUNG and B. S. THOMPSON 1984 *Mechanism and Machine Theory* **19**, 389–396. Material selection: an important parameter in the design of high-speed linkages.
8. J. H. OLIVER, D. A. WYSOCKI and B. S. THOMPSON 1985 *Mechanism and Machine Theory* **20**, 471–482. The synthesis of flexible linkages by balancing the tracer point quasi-static deflections using microprocessor and advanced material technologies.
9. SOONG, D. SUNAPPAN and B. S. THOMPSON 1989 *American Society of Mechanical Engineers Journal Vibration Acoustics, and Reliability in Design* **111**, 430–436. The elastodynamic response of a class of intelligent machinery, part 1: theory.
10. SOONG, D. SUNAPPAN and B. S. THOMPSON 1989 *American Society of Mechanical Engineers Journal Vibration Acoustics, and Reliability in Design* **111**, 437–442. The elastodynamic response of a class of intelligent machinery, part 2: computational and experimental results.
11. C. K. SUNG and Y. C. CHEN 1991 *American Society of Mechanical Engineers Journal of Vibration and Acoustics* **113**, 14–21. Vibration control of the elastodynamic response of high-speed flexible linkage mechanisms.
12. C. Y. LIAO and C. K. SUNG 1993 *American Society of Mechanical Engineers Journal of Mechanical Design* **115**, 658–665. An elastodynamic analysis and control of flexible linkages using piezoceramic sensors and actuators.
13. S. B. CHOI, C. C. CHEONG, B. S. THOMPSON and M. V. GANDHI 1994 *Mechanism & Machine Theory* **29**, 535–546. Vibration control of flexible linkage mechanisms using piezoelectric films.

14. X. M. ZHANG 1999 *Journal of Vibration Engineering* **12**, 93–99. Active residual vibration control for flexible linkage mechanisms.
15. X. M. ZHANG, H. LIU and W. CAO 1996 *Chinese Journal of Mechanical Engineering* **32**, 9–16. Active vibration control of flexible mechanisms.
16. B. S. THOMPSON and X. TAO 1999 *Machine Element and Machine Dynamics De*-71, *The* 1994 *American Society of Mechanical Engineers Design Technique Conferences*, *Minneapolis*, *MN*, September 11–14, 63–69. A note on the experimentally determined elastodynamic response of a slider crank mechanism featuring a macroscopically smart connecting rod with ceramic piezoelectric actuators and strain guage sensors.
17. M. SANNAH and A. SMAILI 1998 *American Society of Mechanical Engineers Journal of Mechanical Design* **120**, 316–326. Active control of elastodynamic vibrations of a four-bar mechanism system with a smart coupler link using optimal multivariable control: Experimental implementation.
18. C. SHAO, X. M. ZHANG and Y. SHEN 2000 *Journal of Sound and Vibration* **234**, 491–506. Complex mode active vibration control of high-speed flexible linkage Mechanisms.
19. C. Q. CHEN and Y. P. SHEN 1997 *Smart Material and Structures* **6**, 403–409. Optimal control of active structures with piezoelectric modal sensors and actuators.
20. X. Q. PENG, K. Y. LAM and G. R. LIU 1998 *Journal of Sound and Vibration* **209**, 635–650. Active vibration control of composite beams with piezoelectrics.
21. K. Y. LAM and T. Y. NG 1999 *Smart Material and Structures* **8**, 223–237. Active control of composite plates with integrated piezoelectric sensors and actuators under various dynamic loading conditions.
22. B. A. FRANCIS 1987 *A Couse in H_∞ Control Theory*. New York: Springer Verlag.
23. J.-S. YANG 1993 *Journal of Guidance*, *Control*, *and Dynamics* **16**, 1131–1137. H_∞ robust control design for linear feedback systems.
24. F. JABBARI, W. E. SCHMITENDORF and J. N. YANG 1995 *Journal of Engineering Mechanics* **121**, 994–1002. H_∞ control for seismic-excited buildings with acceleration feedback.
25. B. WIE and Q. LIU 1993 *Journal of Guidance*, *Control*, *and Dynamics* **16**, 1069–1077. Classical and robust H_∞ control redesign for the Hubble Space Telescope.
26. X. M. ZHANG, J. LIU and Y. SHEN 1996 *Journal of Vibration Engineering* **9**, 99–104. Lower order critical operating speeds identification for flexible linkage mechanisms.